

Simulation of Acoustically Induced Vibrations in a Gas Piping System by a Fluid—Structure Interaction Model

Abdullah Ahmed*, Mennatullah Ramadan*, Mayar Yasser* and
Eslam Reda Lotfy**

Keywords : acoustically induced vibrations, fluid—structure interaction, finite element analysis, modal analysis, harmonic response analysis.

ABSTRACT

The acoustically induced vibrations (AIV) are the vibrations of a piping system by the energy generated by a pressure-reducing device. Such vibrations can resonate with pipe shell vibrating modes. Recently, the capacities of the pressure reducing systems have been increased and some of the piping systems became susceptible to acoustic fatigue failures. In this paper, AIV damage was identified by dynamic stress evaluation at pipe discontinuities (welded connections). This evaluation was performed through a finite element analysis simulation of the fluid—structure coupling. Two types of pipe branching joints were examined for AIV stresses, namely the Weldolet and the Sweepolet. A maximum local stress of 300 MPa was recorded in the Weldolet joint at 1600 Hz excitation frequency, which is ten times the normal-operation stress. This is an indication of the importance of the AIV and the need to consider them at the design stage of the gas piping systems.

INTRODUCTION

Vibration and noise problems due to fluid flow are of great concern in pipeline and piping systems (2019). The Energy Institute (EI) defines the major sources of pipe vibrations (Energy Institute (Great Britain), 2001) as flow induced turbulence, pulsation, mechanical excitation, acoustically induced vibrations,

surge/water hammer, cavitation and flashing.

In large capacity process plants, large sound power generated by pressure reducing devices sometimes result in severe piping vibrations at high frequencies in flare piping systems. These are called Acoustically Induced Vibrations (AIV). High pressure-ratio and mass-flow systems generate high amplitude fluctuating pressures at pressure reducing devices. These dynamic pressure fluctuations propagate downstream and can impart energy to the surrounding structure. The factors affecting noise in a valve are fluid velocity, pressure ratio, mass flow, rate of expansion and contraction, design of the small passages, turns and mutual impingements.

The generated sound pressure field decays downstream the valve and normally dissipates within a ten pipe-diameter distance. The sound pressure field, however, results in acoustic energy propagating downstream the piping as a plane wave together with higher order modes. The important point with the high energy levels in the area immediately downstream the pressure reduction device, within a ten-diameter distance, is that this energy introduces circumferential vibrations in the pipe wall that have the potential to propagate structurally within the piping itself and affect the asymmetric connections in the system, typically the connection to sub-header or header. A structural discontinuity such as a welded Tee fitting creates a stress concentration when the pipe wall vibrates, potentially leading to fatigue failure over time (Eisinger, 1997). Fatigue failures can occur in the process piping or nearby small-bore connections due to the generated broadband sound radiations in the range of 500 Hz to 2000 Hz.

The phenomenon was first reported by Carucci and Mueller (1982) who showed, based on actual failure data, that the AIV failure possibility through a device with high pressure drop and large pipe diameter is related to the sound power generated by the device. Eisinger (1997) proposed an AIV fatigue diagram corresponding to the relations between sound power level and D/h (pipe diameter to wall thickness ratio). The British Energy Institute (EI) (2001) published

Paper Received December, 2020. Revised January, 2021. Accepted February, 2021. Author for Correspondence: E. R. Lotfy [eslam.reda@alexu.edu.eg].

* Undergraduate student, Mechanical Engineering Department, Alexandria University, 21544 Alexandria, Egypt.

** Assistant Professor, Mechanical Engineering Department, Alexandria University, 21544 Alexandria, Egypt.

guidelines for piping vibrations with an evaluation method for the AIV failure probability that is based on the Likelihood-Of-Failure (LOF) concept. The LOF due to AIV is related to the type of branch connection, main pipe to branched pipe diameter ratio, etc. in addition to sound power level and D/h ratio. The EI screening produces an LOF number that defaults for 1 and designates the system to be unsafe if having an LOF of 1 or greater. Systems with an LOF > 1 are at risk and need to be redesigned. An LOF = 0.5 closely fits the basic Carucci/Mueller safe design curve. It is important to remember that the EI guidelines resemble a screening tool rather than a design tool. As explained in the experimental work by Norton (Norton and Karczub, 2007; Norton, 1994), the acoustic energy in the immediate area close to the pressure reduction device are due to an intense non-propagating sound field (turbulence and shock waves).

Many studies (Chadha et al., 2020; Bruce et al., 2013; Nishiguchi et al., 2012; Swindell, 2012) have been devoted to addressing the risk of the AIV such that currently there exists a few protection guidelines. Ghosh et al. (2014) combined Finite Element Analysis (FEA) and modal analysis to a Weldolet, an Insert Weldolet that is a variation of Sweepolet and a Reducing Tee connection in a 24×6 inch Schedule 10S and STD connection under different loading conditions. The effect of the fluid was included implicitly by loading the piping system at the fluid natural acoustic frequencies which were calculated analytically. The results showed that the Reducing Tee has the lowest stress, and the Weldolet has the highest stress value. Kedar and Gulave (2017) utilized CAESAR II to prove the effectiveness of the EI guidelines in reducing the LOF due to AIV in gas piping systems. Dweib (2011, 2012) presented an approach for the application of the finite element method to the estimation of the dynamic stresses at different piping components subjected to AIV, taking into consideration the fluid—structure interaction. Nishiguchi et al. (2014) investigated experimentally the combined effect of acoustically induced vibrations and flow induced vibrations on a Tee in a flare piping system.

Many published standards (e.g. Energy Institute (Great Britain), 2001) provide guidelines for different types of branch connections. Recently, FEA research (Liu et al., 2016; Prakash et al., 2015; Lin et al., 2014) developed the design curve for Sweepolets. Although welded supports are commonly considered as potential AIV failure locations, there are many gaps and inconsistencies among the published standards and guidelines regarding the design limit and mitigation options, especially for the supports with partial reinforcement pads whose the design curve and fatigue life remain unknown. Some researchers suggested treating them as Weldolets because they both utilize fillet weld; some others excluded them from the AIV analysis due to the lack of knowledge; and the

remainders suggested treating them as Sweepolets.

Reasonable research was conducted in favor of enhancing the AIV damage evaluation method. However, the effect of fluid properties and acoustic wave type on the response of the piping have rarely been addressed. The response of the piping as displacement and dynamic stresses is a function of the acoustic pressure fluctuation at the points of pressure reduction as well as the characteristics of the fluid—structure system. The target of the present research was to build a more realistic model which accounts for the acoustic wave behavior by coupling the fluid and solid bodies in the simulation. The model was applied to branch connections of types Weldolet and Sweepolet. The main area of interest in the present investigation is the dynamic structural response of the piping components in presence of an acoustic source of excitation. The fatigue failure assessment was presented here in order to indicate the method of application of the results of the dynamic analysis. This fatigue failure assessment was based on the cumulative damage criteria as provided in the ASME code for pressure vessel design (Miller, 2002).

METHOD

The analysis was mainly conducted using numerical techniques.

Finite Element Analysis

The use of FEA to solve acoustic problems enables investigating complex situations that would otherwise be too cumbersome or time consuming to solve using analytical methods. Analytical methods are only suitable for solving regular-shaped objects such as ducts, hard-walled rectangular cavities, and so on. The finite element analysis considers the Fluid—Structure Interaction (FSI). The loading associated with the input acoustic energy was introduced in terms of particle velocity calculated from the Sound Pressure Level (*SPL*).

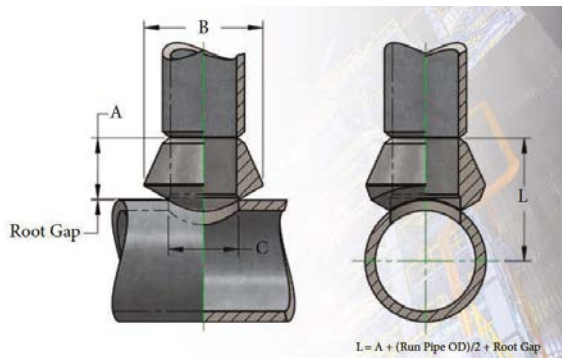
In the present research, the finite element model was applied to a straight pipe with a single small-bore connection. Welding joint geometry details were modeled by SOLIDWORKS® software and imported to ANSYS® software to conduct the simulation. The geometry consisted of two bodies, the first was the solid body and contains all the details of the welding junctions, and the second was the acoustic body and inherited the properties of acoustic media (fluid). This type of analysis uses ANSYS FEA with ACOUSTICS ACT extension to account for fluid—structure interaction. The modal analysis was used to investigate the vibrating modes and the corresponding frequencies of the two bodies, then harmonic response analysis was held by applying loads at different excitation frequencies to calculate the Von-Mises peak stress over the range of frequencies from 500 to 2000 Hz.

Configuration Model

The critical locations in the piping system that are prone to AIV failure (Energy Institute (Great Britain), 2001) are branch connections, welded pipe supports, relief valves, control valves, small branch connections, pressure reducing valves, restrictive orifice plates, recycling valves and high flow rate piping. On these grounds, two geometrical models were tested in this research; each comprises a pipe with a Tee branch. The main dimensions of each are listed in Table 1. The difference between the two configurations is the joint method; in one configuration, the Weldolet joint was applied and in the second the Sweepolet was applied. Dimensioned configurations are shown in Figs. 1 and 2, respectively. The geometries as constructed by SOLIDWORKS are illustrated in Figs. 3 through 5. The fluid considered in the analysis was methane to match the conditions in real gas piping systems. The pipe was supported at both ends by fixed displacement supports that do not allow the motion in the radial direction.

Table 1. Dimensions of the main and branched pipes.

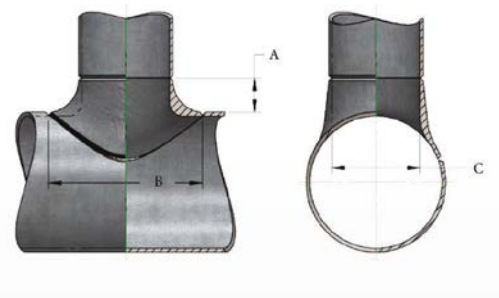
Main pipe diameter	0.4 m (16")
Main pipe thickness	0.0214 m (0.843")
Main pipe length	10 m (32.8')
Branch diameter	0.0254 m (1")
Branch thickness	0.015 m (0.179")
Branch length	0.2 m (7.87")



NPS 16

A	0.1064 m (4 3/16 ")
B	0.061 m (2.4")
C	0.381 m (15")

Fig. 1. The geometry and dimensions of the Weldolet joint (Reducing Extra Strong).



NPS 16

A	0.09525 m (3 3/4 ")
C	0.7112 m (28")

Fig. 2. The geometry and dimensions of the Sweepolet joint (Butt-Weld Insert Reinforcement).

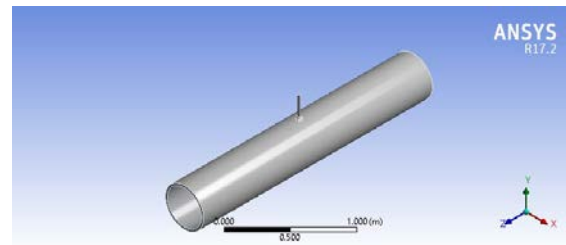


Fig. 3. The geometry of the pipe.

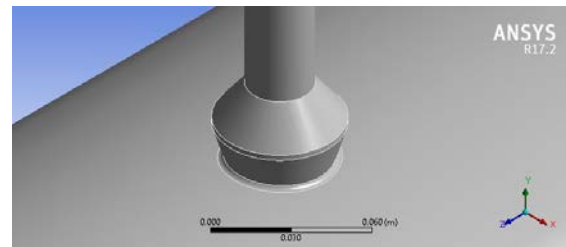


Fig. 4. A closeup of the geometry of Weldolet connection.

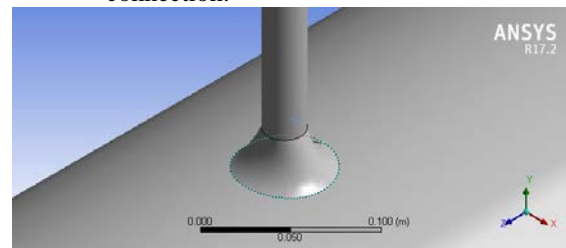


Fig. 5. A closeup of the geometry of Sweepolet connection.

Governing Equations

In acoustic FSI problems, the structural dynamics equation must be considered alongside with the flow momentum and continuity equations. The discretized structural dynamics equation can be formulated using the structural elements. The Navier-Stokes momentum equations and continuity equations

are simplified to get the acoustic wave equation using the following assumptions:

- The fluid is compressible (density changes due to pressure variations).
- The speed of the acoustic wave is much higher than the flow velocity. Therefore, the mean fluid flow was ignored.

The resulting momentum equation is presented below.

$$\nabla \cdot \left(\frac{1}{\rho_o} \nabla p \right) - \frac{1}{\rho_o c^2} \frac{\partial^2 p}{\partial t^2} + \nabla \cdot \left[\frac{4\mu}{3\rho_o} \nabla \left(\frac{1}{\rho_o c^2} \frac{\partial p}{\partial t} \right) \right] = - \frac{\partial}{\partial t} \left(\frac{Q}{\rho_o} \right) + \nabla \cdot \left[\frac{4\mu}{3\rho_o} \nabla \left(\frac{Q}{\rho_o} \right) \right]. \quad (1)$$

Boundary Conditions

Non-reflective boundary was assigned to both ends of the pipe and closed end was assigned to the branch. It was required to define the sound pressure level (*SPL*) at inlet, however, this was not applicable in the used software. The solution was to translate the *SPL* to particles velocity or mass source. The flow was powered by an inlet acoustic surface-normal velocity (particles velocity). The particles velocity (*V*) was obtained from sound amplitude pressure (*AP*), fluid density (ρ) and speed of sound (*c*) through,

$$V = \frac{AP}{\rho \times c}. \quad (2)$$

The sound amplitude pressure *AP* (peak pressure) inside the pipe was obtained from *SPL* through,

$$AP = \sqrt{2} P_{\text{rms}}, \quad (3)$$

$$P_{\text{rms}}^2 = P_{\text{ref}}^2 \times 10^{\frac{SPL}{10}}, \quad (4)$$

$$P_{\text{ref}} = 2 \times 10^{-5} \text{ Pa}. \quad (5)$$

Based on Eqs. 2 through 5, and assuming a 175-dB *SPL*, the acoustic surface-normal velocity was assigned an amplitude of 78.17 m/s.

It is worth mentioning that the acoustic surface-normal velocity would also be calculated from the sound power level (*SWL*, Watt) generated by the pressure reducing component as given below,

$$SWL = 10 \log \left[M^2 \left(\frac{P_1 - P_2}{P_1} \right)^{3.6} \left(\frac{T_1}{W} \right)^{1.2} \right] + 126.1, \quad (6)$$

$$P_{\text{rms}}^2 = SWL_{\text{ref}} \times 10^{\frac{SWL}{10}} \frac{\rho c}{A}, \quad (7)$$

$$SWL_{\text{ref}} = 10^{-12} \text{ Watt}, \quad (8)$$

where, *A* is the pipe cross-sectional area.

Acoustic Analysis

The ANSYS® package was used to build the mesh and undertake the simulations. The ACT Acoustics extension add-on was employed to conduct the acoustic analyses. The add-on installs a new menu bar in the mechanical acoustic analysis module. Typical quantities of interest are the pressure distribution in the fluid at different frequencies, pressure gradient, particle velocity, sound pressure level, as well as scattering, diffraction, transmission, radiation, attenuation, and dispersion of acoustic waves.

Modal Analysis

The goal of modal analysis was to determine the standing wave patterns within the structure corresponding to the expected range of load frequencies. A coupled acoustic analysis takes the fluid—structure interaction into account. The acoustic model used was an uncoupled acoustic analysis model, which separately simulated the fluid and pipe shell and ignored any fluid—structure interactions. The program assumed the fluid to be compressible but allowed relatively minor pressure changes with respect to the mean pressure. Also, the fluid was assumed to be non-flowing. The model calculated the pressure deviation from the mean pressure, rather than the absolute pressure. For pure acoustic modal analysis, the acoustic modes were computed using the following equation,

$$(-\omega^2[M] + j\omega[C] + [K])\{p\} = 0, \quad (9)$$

where, [*M*] is the mass matrix, [*C*] is the damping matrix, [*K*] is the stiffness matrix, {*p*} is the vector of nodal pressures for an acoustic system or displacements for a structural system.

The pipe and flow were studied separately. The mesh was carefully constructed to be able to capture the mode shapes of the structure. For linear elements, at least 12 elements per wavelength are needed, while 6 elements per wavelength are needed for quadratic elements (Marburg, 2002). The mesh specs in each case is represented in Table 2. As shown in Figs. 6 and 7, the pipe and fluid vibration modes coincide at frequencies less than 600 Hz. Beyond this frequency, the trend of fluid vibrating modes becomes very steep.

Table 2. Mesh element size in modal analysis.

		Maximum element size (mm)	Number of elements
Weldolet	Pipe	127	88,838
	Fluid	127	78,711
Sweepolet	Pipe	63.58	81,620
	Fluid	63.29	78,668

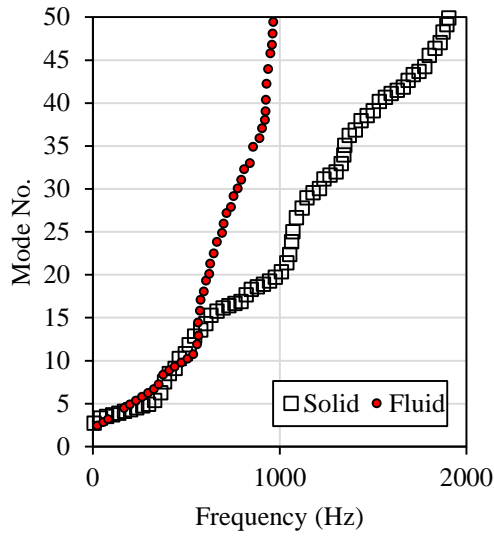


Fig. 6. Natural frequency range of the Weldolet joint.

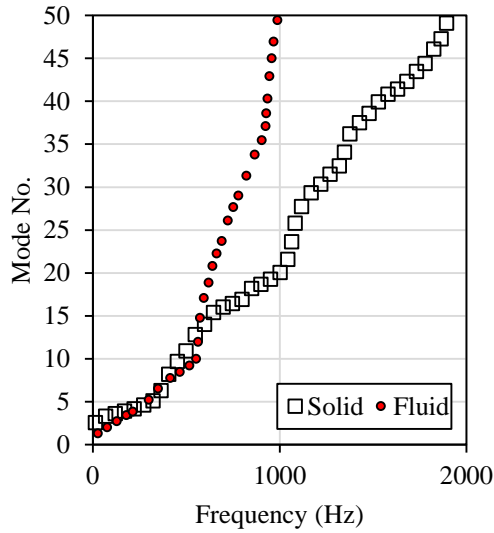


Fig. 7. Natural frequency range of the Sweepolet joint.

Harmonic Response Analysis

The objective of a harmonic analysis was to calculate the response of the coupled systems (pipe and fluid) to a variable flow rate or pressure excitation at specific frequencies. This technique was used by Wu et al. (2021) to study the response of vortex induced vibrations in strake-covered pipelines. Also, Zhao et al. (2021) utilized harmonic analysis to test vibration control methods in a hydraulic power system. In harmonic response analysis for pure acoustic problems, the following equation is resolved:

$$(-\omega^2[M] + j\omega[C] + [K])\{p\} = \{F\}, \quad (10)$$

where, $\{F\}$ is the acoustic or structural load.

The interaction of the fluid and the structure at mesh interface means the acoustic pressure exerts a force on the structure while the structural motions produce an effective “fluid load”. The governing finite element equation matrix then becomes,

$$[M_s]\{\ddot{U}\} + [K_s]\{U\} = \{F_s\} + [R]\{P\}, \quad (11)$$

$$[M_f]\{\ddot{P}\} + [K_f]\{P\} = \{F_f\} - \rho_0[R]^T\{\ddot{U}\}, \quad (12)$$

where, $[K_s]$ is the structural stiffness matrix, $[M_s]$ is the structural mass matrix, $\{F_s\}$ is a vector of applied structural loads, $\{U\}$ is a vector of unknown nodal displacements and hence $\{\ddot{U}\}$ is a vector of the second derivative of displacements with respect to time, and $[R]$ is the coupling matrix that accounts for the effective surface area associated with each node on the fluid—structure interface, $[K_f]$ is the equivalent fluid stiffness matrix, $[M_f]$ is the equivalent fluid mass matrix, $\{F_f\}$ is a vector of applied fluid loads, $\{P\}$ is a vector of unknown nodal acoustic pressures, and $\{\ddot{P}\}$ is a vector of the second derivative of acoustic pressure with respect to time.

Tetrahedral mesh was chosen for the analysis to enable capturing the fine connection details. The meshes of the two cases are demonstrated in Figs. 8 and 9. The applied mesh passed a grid-independence test involving maximum stress computation at 500 Hz frequency, which verifies the fidelity of the present conclusions. The test included four mesh sizes, namely, 80, 120, the current 190, and 350 thousand cells. The results of the grid-dependency analysis are illustrated in Figs. 10 and 11. The figures show the variation of the stress (Fig. 10) and error relative to the next finer mesh (Fig. 11).

Table 3. Mesh element size in harmonic analysis.

	Maximum element size (mm)	Number of elements
Weldolet	25	189,336
Sweepolet	24	209,921

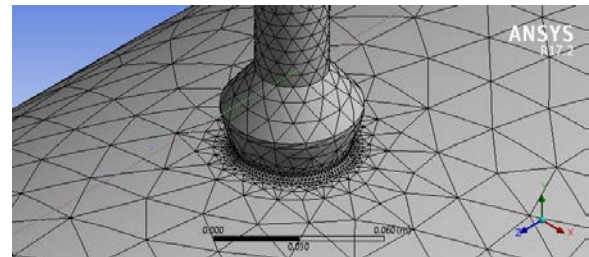


Fig. 8. Mesh around the welding joint of the Weldolet connection.

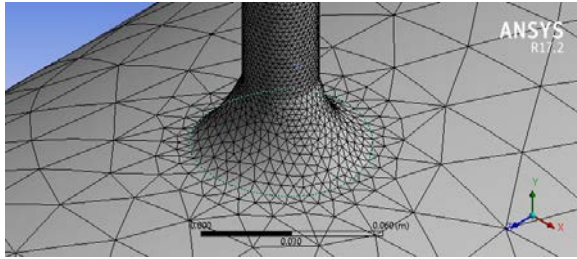


Fig. 9. Mesh around the welding joint of the Sweepolet connection.

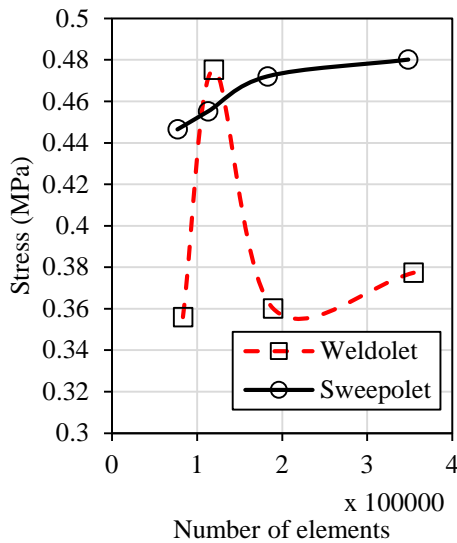


Fig. 10. Mesh dependency analysis; stress at 500 Hz against number of cells.

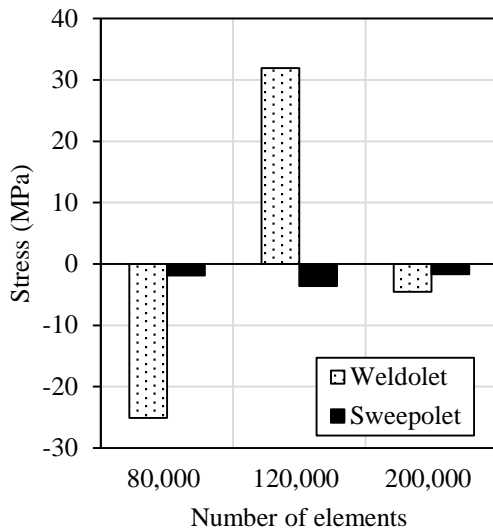


Fig. 11. Mesh dependency analysis; error in stress with respect to the next finer mesh.

As aforementioned, the boundary conditions were set as fixed displacement on both ends of the

main pipe, non-reflecting boundaries on both ends of fluid body in the main pipe and closed boundary on the end of fluid in branch connection. The acoustic source on the fluid body at the inlet of the main pipe was defined by surface-normal velocity with amplitude of 78.17 m/s, as calculated from Eqs. 2 through 5.

RESULTS AND DISCUSSION

As indicated by the stress distribution in Figs. 12 through 15, the maximum stress took place at the small-bore connection and never was recorded in the straight pipe. This was basically attributed to the circumferential discontinuity of the pipe at the connection point. According to this analysis, this was not the only reason; it was found that in both joint types, the acoustic wave behaved as a longitudinal wave in the main pipe whereas in the branch the wave reflected from the closed end and converted to a standing wave. Therefore, the peak pressure in the branch connection was double that in main pipe as shown in Figs. 16 through 19. In summary, the stress concentrated at the welding joint due to the difference between the small and main pipes in load and mode of deformation.

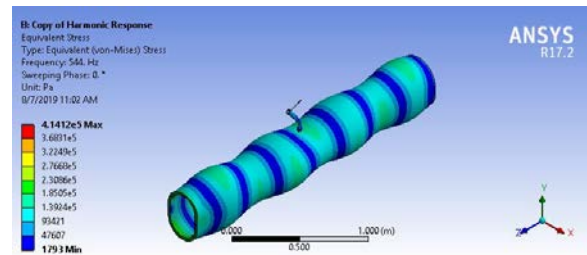


Fig. 12. Stress distribution on the pipe at 544 Hz in the Weldolet configuration.

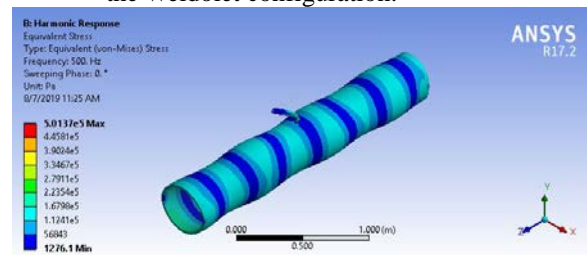


Fig. 13. Stress distribution on the pipe at 544 Hz in the Sweepolet configuration.

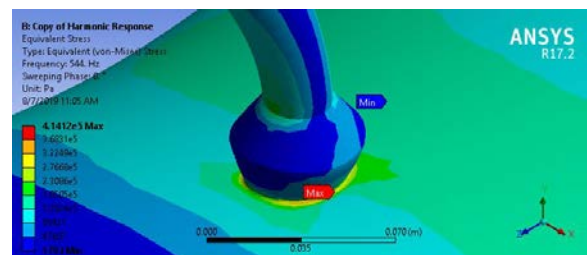


Fig. 14. Stress distribution on the Weldolet joint at 544 Hz.

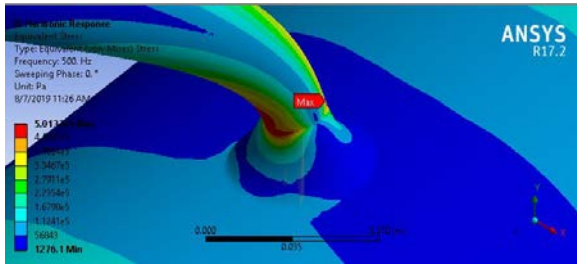


Fig. 15. Stress distribution on the Sweepolet joint at 544 Hz.

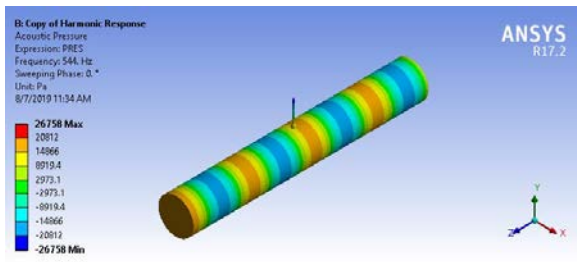


Fig. 16. Pressure distribution on the pipe at 544 Hz and 176 dB in the Weldolet configuration.

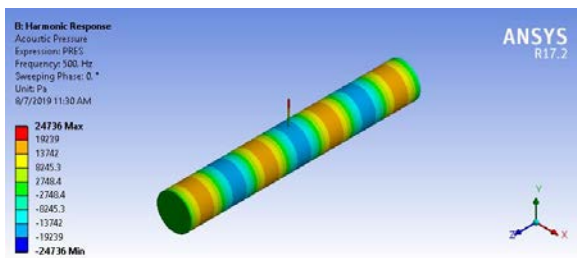


Fig. 17. Pressure distribution on the pipe at 544 Hz and 176 dB in the Sweepolet configuration.

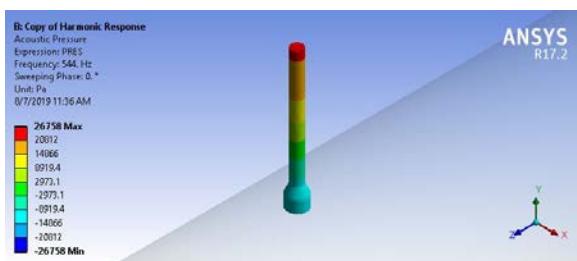


Fig. 18. Pressure distribution on the branch in the Weldolet configuration.

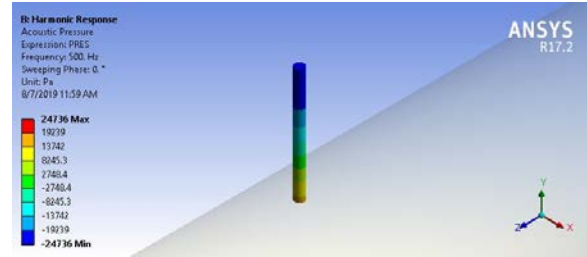


Fig. 19. Pressure distribution on the branch in the Sweepolet configuration.

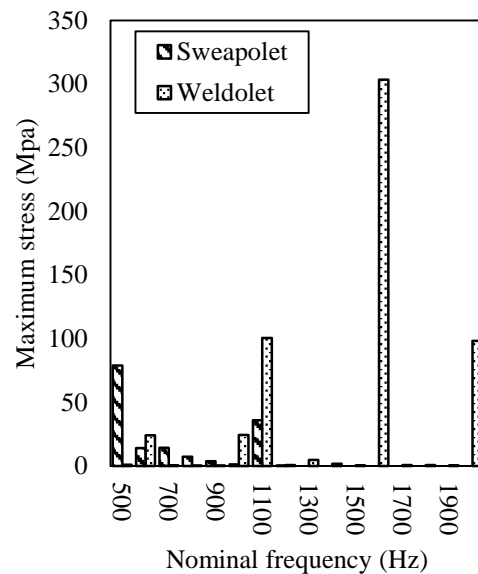


Fig. 20: A comparison between the stresses in the two branch connections at the same frequency.

According to Figs. 14 and 15, the maximum local stress on the branch occurred at the welding between the main pipe and the connection in case of the Weldolet configuration, and at the root of the branch itself in the Sweepolet configuration. As can be noticed in Fig. 20, the Weldolet joint produced a higher maximum local stress under most of the excitation frequencies. For the examined configuration, the worst case for the Weldolet joint was recorded around 1600 Hz (~300 MPa), and for the Sweepolet around 500 Hz (~75 MPa). Moreover, stress minor spikes were noticed at 1100 and 2000 Hz. The effect of resonance between the modes of the fluid and pipe shell at low frequencies (< 600 Hz, refer to Figs. 6 and 7) appear in Fig. 20 as elevated stresses at this range. The difference between the two geometries justified the occurrence of the resonance at disparate frequencies and unique locations. The resonance in the Sweepolet configuration at 500 Hz caused the stress to exceed the corresponding stress in the Weldolet configuration at the same frequency. The stress reported in the Weldolet branch exceeded the yield

stress of the material which is an alert of a probable failure of the branch if subjected to such a frequency for a sufficiently long period. These values of stress coincide with the data presented by Liu et al. (2016) for harmonic analysis of similar branched connections, where the stress reached as high values as 172 MPa in a Sweepolet connection and 283 MPa in a Sockolet connection. Table 4 compares the present results and data reported in the literature for harmonic analysis of AIV in branched pipe connections. The table displays that the current results fall well within the range of the reported data which gives a credit to the current analysis.

Table 4: Results from the present study and the literature of the maximum stress in branched pipe connections.

	Present research	Liu et al. (2016)	Lin et al. (2014)	Nishiguchi et al. (2014)
Method of analysis	CFD	CFD	CFD	Experimental
Pipe diameter (D, inch)	16	16	24	6
Branch diameter (inch)	1	1	0.75	0.75
Pipe wall thickness (h, inch)	0.843	0.5	0.375	1.1
Type of connection	Sweepolet / Weldolet	Sweepolet / Sockolet	Sweepolet / Sockolet	90-degree branched connection
Maximum stress (MPa)	78.86 / 303.4	172 / 283	262 / 476	~ 30
Maximum stress $\times \frac{h}{D}$	4.15 / 16	5.4 / 8.8	4.1 / 7.4	5.5
Frequency of Sound Pressure associated with maximum stress (Hz)	~ 500 / 1600	--	--	~ 1000

Several techniques are suggested to protect the system from failure due to AIV including, but not limited to, reducing the AIV source pressure drop, reinforcing the main pipe or increasing its thickness, using acoustic silencers, and minimizing circumferential discontinuities.

CONCLUSIONS

Acoustically induced vibrations can cause serious and costly failures in gas piping systems. The current piping design methodology does not account for AIV. Moreover, the codes and standards do not include a robust evaluation technique for the built structures. The objective of this research was to examine a new method to evaluate AIV in gas piping systems. The study case was a branched piping system with two types of connections, namely, the Weldolet

and the Sweepolet. The system was subjected to modal analysis and harmonic analysis. The range of acoustic frequencies applied to the system was between 500 Hz and 2000 Hz. The following conclusions were deduced:

- A range of coincidence in acoustic modes between the fluid and the pipe shell was noticed at excitation frequencies less than 600 Hz in the Weldolet and Sweepolet configurations.
- The maximum stress was noticed at the welding between the main pipe and the connection in case of the Weldolet and at the root of the branch itself in case of the Sweepolet.
- The peak maximum local stress in case of the Weldolet was recorded at 1100 Hz frequency and exceeded 300 MPa. On the other hand, the Sweepolet connection showed a smaller peak of 75 MPa at 500 Hz.

CONFLICTS OF INTEREST

The authors declare no conflict of interest.

REFERENCES

- Bruce, R.D., Bommer, A.S., and LePage, T.E., "Solving acoustic-induced vibration problems in the design stage,"; *Sound Vib.*, Vol. 47, No. 8, pp. 8–11 (2013).
- Carucci, V.A., and Mueller, R.T., "Acoustically Induced Piping Vibration in High Capacity Pressure Reducing Systems.,"; *Am. Soc. Mech. Eng.* (1982).
- Chadha, A., Li, W., Desai, P., and Thomas, D., "Investigating Piping Acoustic Induced Vibration Problems and Current Assessment Methods to Evaluate Fatigue Life,"; *INTER-NOISE NOISE-CON Congr. Conf. Proc.*, pp. 1003–1015 (2020).
- Dweib, A.H., "Acoustic fatigue assessment of piping system components by finite element analysis,"; *Am. Soc. Mech. Eng. Press. Vessel. Pip. Div. PVP*, Vol. 3, pp. 203–214 (2011).
- Dweib, A.H., "Power Spectral Density analysis of acoustically induced vibration in piping systems,"; *Am. Soc. Mech. Eng. Press. Vessel. Pip. Div. PVP*, Vol. 3, pp. 111–117 (2012).
- Eisinger, F.L., "Designing piping systems against acoustically induced structural fatigue,"; *J. Press. Vessel Technol. Trans. ASME*, Vol. 119, No. 3, pp. 379–383 (1997).
- Energy Institute (Great Britain), *Guidelines for the avoidance of vibration induced fatigue in process pipework Offshore Res. Focus*, Energy Institute, No. 131 (2001).
- Ghosh, A., Niu, Y., and Arjunan, R., "Difficulties in predicting cycles of failure using finite

- element analysis of acoustically induced vibration (AIV) problems in piping systems,"; Am. Soc. Mech. Eng. Press. Vessel. Pip. Div. PVP, Vol. 3 (2014).
- Goridko, K., Khabibullin, R., and Verbitsky, V., "Flow induced vibration and movements modelling on multiphase pipeline on Russian far north green field,"; Soc. Pet. Eng. - SPE/IATMI Asia Pacific Oil Gas Conf. Exhib. 2019, APOG 2019 (2019).
- Kedar, B.B., and Gulave, J.S., "Acoustically Induced Vibration (AIV) & Flow Induced Vibration (FIV) Analysis for the High Pressure Reducing Systems using Energy Institute Guidelines,"; J. Res. Vol., Vol. 02, No. 11, pp. 10–13 (2017).
- Lin, D., Prakash, A., Diwakar, P., and David, B., "Acoustic fatigue evaluation of branch connections,"; Am. Soc. Mech. Eng. Press. Vessel. Pip. Div. PVP, Vol. 3 (2014).
- Liu, Y., Diwakar, P., Lin, D., Eljaouhari, I., and Prakash, A., "Development of design curve for sweepolet subjected to acoustic induced vibration,"; Am. Soc. Mech. Eng. Press. Vessel. Pip. Div. PVP, Vol. 3 (2016).
- Marburg, S., "Six boundary elements per wavelength: Is that enough?,"; J. Comput. Acoust., Vol. 10, No. 1, pp. 25–51 (2002).
- Miller, U.R., Section VIII Division 1: Rules for construction of pressure vessels ASME Boil. Press. Vessel Code, Vol. 2 (2002).
- Nishiguchi, M., Izuchi, H., Hayashi, I., and Minorikawa, G., "Investigation of pipe size effect against AIV,"; 41st Int. Congr. Expo. Noise Control Eng. 2012, INTER-NOISE 2012, Vol. 10, pp. 8709–8720 (2012).
- Nishiguchi, M., Izuchi, H., and Minorikawa, G., "Investigation of characteristic of flow induced vibration caused by turbulence relating to acoustically induced vibration,"; Am. Soc. Mech. Eng. Press. Vessel. Pip. Div. PVP, Vol. 3 (2014).
- Norton, M.P., "Acoustically Induced Structural Vibration and Fatigue—A Review,"; Acoust. Induc. Struct. Vib. Fatigue-A Rev., Vol. 1, No. Proceedings of Third International Congress on Air and Structure-Borne Sound and Vibration, Montreal, Canada, pp. 147–166 (1994).
- Norton, M.P., and Karczub, D.G., Fundamentals of Noise and Vibration Analysis for Engineers, 2nd Edition Noise Control Eng. J., Cambridge university press, Vol. 55, No. 2 (2007).
- Prakash, A., Deane, P., Diwakar, P., Liu, Y., Lin, D., and Jaouhari, M., "Acoustic vibration induced fatigue in pipe joints,"; Am. Soc. Mech. Eng. Press. Vessel. Pip. Div. PVP, Vol. 3 (2015).
- Swindell, R., "Acoustically induced vibration - Development and use of the 'Energy Institute' screening method,"; 41st Int. Congr. Expo. Noise Control Eng. 2012, INTER-NOISE 2012, Vol. 10, pp. 8721–8728 (2012).
- Wu, J., Yin, D., Passano, E., Lie, H., Peek, R., Sequeiros, O.E., Ang, S.Y., Bernardo, C., and Aienza, M., "Forced Vibration Tests for In-Line Vortex-Induced Vibration to Assess Partially Strake-Covered Pipeline Spans,"; J. Offshore Mech. Arct. Eng., Vol. 143, No. 3 (2021).
- Zhao, J., Sun, W., Wang, X., Sang, Y., and Liu, P., "Fluid-structure interaction analysis of the return pipeline in the high-pressure and large-flow-rate hydraulic power system,"; Prog. Comput. Fluid Dyn. An Int. J., Vol. 21, No. 1, p. 38 (2021).

NOMENCLATURE

- A*: pipe cross-sectional area (m²)
- c*: speed of sound ($\sqrt{\frac{K}{\rho_0}}$) in fluid medium (m/s)
- D*: pipe diameter (m)
- h*: pipe wall thickness (m)
- m*: mass source rate (kg/m²-s)
- M*: mass flow rate (kg/s)
- K*: bulk modulus of elasticity of fluid (Pa)
- P*: acoustic pressure field (Pa)
- P_{ref}*: reference pressure (Pa)
- P_{rms}*: root mean square value of pressure (Pa)
- P_a*: amplitude pressure (peak Pressure, Pa)
- P₁*: upstream pressure (Pa)
- P₂*: downstream pressure (Pa)
- Q*: volume flow rate from the mass source in the continuity equation (m³/s)
- SPL*: sound pressure level (dB)
- SWL*: sound power level (Watt)
- t*: time (s)
- V*: particles velocity (m/s)
- T*: temperature (K)
- W*: gas molecular weight (kg/ kmole)
- μ*: gas dynamic viscosity (Pa.s)
- ρ₀*: mean fluid density (kg/m³)
- ρ*: fluid density field (kg/m³)
- ASME: American Society for Mechanical Engineers
- AIV: Acoustically Induced Vibrations
- CFD: Computational Fluid Dynamics
- LOF: Likelihood-Of-Failure
- EI: Energy Institute
- FEA: Finite element analysis
- FSI: Fluid—Structure Interaction